Available online at www.sciencedirect.com

SciVerse ScienceDirect

Procedia Materials Science 1 (2012) 156 – 163

Procedia Materials Science

www.elsevier.com/locate/procedia

11th International Congress on Metallurgy & Materials SAM/CONAMET 2011.

On the Al content and characterization of $MmNi_{5-x}Al_x$ synthesized by mechanical alloying

S. A. Obregón[a,b,c,*], J. Andrade Gamboa[a,c], M. R. Esquivel[a,c,d]

[a] *Centro Atómico Bariloche, Comisión Nacional de Energia Atómica, Bustillo km. 9.5, Bariloche, Argentina.*
[b] *Instituto Balseiro, Universidad Nacional de Cuyo (UNCu), Bustillo km. 9,5, Bariloche, Argentina.*
[c] *CRUB, Universidad Nacional del Comahue (UNCo), Quintral 1250, Bariloche, Argentina.*
[d] *Consejo Nacional de Investigaciones Científicas y Técnicas (CONICET), Argentina*

Abstract

The development of new technologies applied to hydrogen thermal compression is oriented to the design of reversible hydride forming compounds that reach the desired pressure conditions by modifying the temperature. Particularly, the main efforts are focused on the research of multi substituted AB_5 compounds.
In this work, three mixtures of $Mm/(5-x_n)Ni/(x_n)Al$ (Mm= Mischmetal $=La_{0.25}Ce_{0.52}Nd_{0.17}Pr_{0.06}$) with nominal composition x_n = 0.5, 0.75 and 1 were milled by low energy reactive milling to synthesize the intermetallic of composition $MmNi_{5-x}Al_x$. Samples were annealed under Ar atmosphere at 600 ºC for 24 h. The structure and microstructure were characterized by X-ray powder diffraction (XRD). The content x of Al in the AB_5 structure was calculated by means of a geometrical model developed under the hypothesis of rigid spheres. The effect of annealing on the microstructure for each nominal composition was analyzed. Minor Mm-Ni phases formed were quantified. The results of this work are framed within a project including the synthesis and optimization of materials applied to the development of multi stage thermal compressors.

AB_5, Hydrogen, Compression

* Corresponding author. Tel.: +54 294 444 5139; fax: +54 294 444 5290.
E-mail address: obregon@cab.cnea.gov.ar

2211-8128 © 2012 Published by Elsevier Ltd. Selection and/or peer-review under responsibility of SAM/CONAMET 2011, Rosario, Argentina.
Open access under CC BY-NC-ND license. doi:10.1016/j.mspro.2012.06.021

1. Introduction

Reactive milling is a technique formerly used in the ceramic industry [Suryanarayana, 2001]. It is applied to the elaboration of new materials due to its versatility and capability to obtain products under different atmospheres in a wide temperature range. The synthesis of intermetallics is worthy of mention [Koch et al., 1996]. In case of AB_5 intermetallics, where A is a lanthanide/alloy and B is an element of groups 3 to 15, the synthesis by reactive milling becomes in an excellent alternative over fusion methods. The advantage includes stoichiometry control and possibility of scaling up to industrial level [Liang et al., 2001; Simičić et al., 2001; Jurczyk et al., 2002; Esquivel et al., 2007]. Moreover, the use of this technique near room temperature followed by annealing at intermediate temperatures (T < 600 ºC), reduces the technical requirements of devices used for high temperature methods (T > 700 ºC).

The development of materials for hydrogen thermal compression focuses primarily on the design, synthesis and characterization of multi-substituted AB_5 intermetallics. It is based on the close correlation between the change of structural properties associated with compositional changes, attributable to different identities of A and B elements or alloys, with changes in the thermodynamic properties of hydrogen sorption. This fact occurs because the plateau pressure, correlated with the equilibrium pressure due to the formation of the hydride to a given P and T, is inversely related to the intermetallic cell volume [Magee et al., 1981; Mediema, et al., 1983].

In a previous work about synthesis of $MmNi_{5-x}Al_x$ intermetallics [Obregón et al., 2012] four characteristic stages of the process as a function of integrated milling times, t_{im}, were identified: Initial stage ($0 < t_{im} < 20$ h), intermediate stage (20 h $< t_{im} < 40$ h), final stage (40 h $< t_{im} < 120$ h) and completion stage ($t_{im} > 120$ h). It was also shown that imrovement of final intermetallic can be achieved after annealing at a temperature of 500 ^oC, a value at least 100 ^oC lower than the lowest one reported for these systems [Obregón et al., 2012, Liang et al., 2001].

Application for hydrogen thermal compression requires an accurate knowledge of the intermetallic composition. This feature is needed to estimate the maximum capacity of the sample and the possible compression ratio (R_c).The degree of substitution of the alloying element in the intermetallic cannot be correctly measured by means of chemical analysis techniques such as energy dispersive spectroscopy because the total elemental composition of the sample is measured, instead. Therefore, the possible presence of minor phases might prevent to correlate the measured sample composition to the correct AB_5 stoichiometry. These phases may be formed irrespective of the synthesis method or due to an incomplete synthesis reaction.

Provided there is either an empirical or a theoretical structural model to quantify compositional changes, this problem can be solved for a given phase using X-ray diffraction even in the presence of other phases. This possibility expands the capability of this technique allowing a simultaneous quantitative phase analysis.

In this work, it is presented an analysis on the synthesis and characterization of the Al content in $MmNi_{5-x}Al_x$ intermetallics with several nominal compositions. An ad hoc structural model is developed. The model correlates cell parameters to x, the degree of substitution of Al in the AB_5 structure. The results offer accurate and relevant information for the design of single and multi-stage hydrogen thermal compressors. This objective aimed the elaboration of this work.

2. Experimental

A mixture of Ni (Sigma / Aldrich, 99.99%, -100 mesh), Mm = $La_{0.25}Ce_{0.52}Nd_{0.17}Pr_{0.06}$ (Reacton, 99.6%) and Al (Aldrich, 99.99%, 100 μm flakes), along with stainless steel balls were placed in a stainless steel chamber under Ar atmosphere. The mixture was alloyed by reactive milling in a mill UNI-BALL-MILL II (Australian Scientific Instruments). A ratio of mass of balls / mass of sample (R) of 11.2 was chosen for this process. The

milled samples were annealed under Ar atmosphere at different temperatures. Handling was done under controlled oxygen (>0.01 ppm) and humidity (>0.01 ppm) contents in a glove box (Mbraum II, Unilab).

Three mixtures $Mm/(5-x_n)Ni/(x_n)Al$ with nominal composition x_n = 0.5, 0.75 and 1 were milled up to the completion stage. Then, samples were thermally treated 24 h in Ar atmosphere at 600 ^oC.

The samples were analyzed by X-ray powder diffraction (XRD) at room temperature on a Phillips instrument PW1710/01, K_α radiation of Cu (graphite monochromator).

3. Results and Discussion

The X-ray diffractograms for the three samples are qualitatively similar with a high signal to background ratio appropriated to estimate accurately the cell parameters from peak position. Figure 1 shows the one corresponding to x_n = 1. In addition to $MnNi_{5-x}Al_x$, the presence of minor phases, including Mn_7Ni_3 and residual Ni are observed.

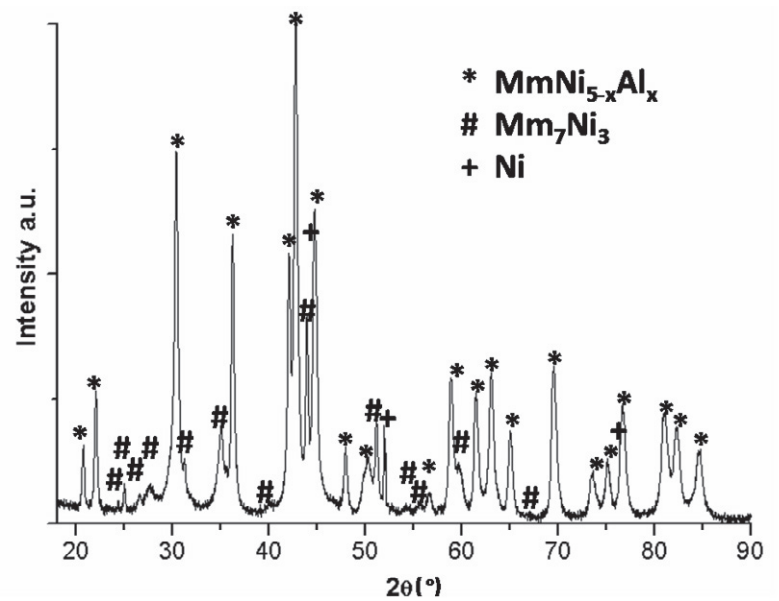

Figure 1: X-ray diffractogram of sample with x_n = 1.

The crystallite size, D, and micro strain, ε, for $MmNi_{5-x}Al_x$ (table 1) were calculated using the method of single peak [Langford et al., 1988] based on 110 reflection. Results are summarized in Table 1. Microstructural values are consistent with samples annealed at intermediate temperatures [Obregón et al., 2012]. Values are not as large as in samples obtained by high temperature synthesis methods [Ares et al., 2005] but appropriate for application to thermal hydrogen compression [Esquivel and Rodriguez, 2009].

In a general tendency, it is observed that microstructural values are of the same order of magnitude independently of the nominal composition x_n. This result indicates that annealing conditions should be the same for all AB_5´s. It implies a generalization for these conditions with no further need of analysis for samples with other degrees of substitution. It is a very relevant result because homogenization of synthesis-improvement conditions results in reduced manufacture costs.

Table 1: Microstructural parameters for $MmNi_{5-x}Al_x$

x_n	D_{110} (nm)	ε_{110} (%)
0.5	50	0.4
0.75	60	0.3
1	40	0.2

Despite the generalization of the annealing conditions, it is important to verify if the nominal content of Al added to the milling chamber (x_n) is equivalent to the final stoichiometry of the AB_5. This measurement is a correlation between the nominal (x_n) and experimental (x) degrees of substitution of Al in the AB_5. To determine the Al content in $MmNi_{5-x}Al_x$, it was developed a geometric-crystallographic model of AB_5 unit cell. The model is schematized in figure 2 (space group *P*6/*mmm*, Wyckoff positions: A @ 1*a*, B @ 2*c* and 3*g*).

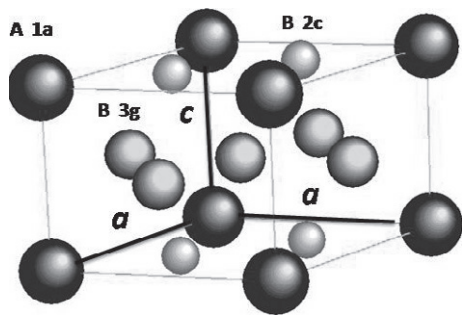

Figure 2: AB_5 cell

This model is based on the assumption of hard spheres that fit into the structure. The effective radius R^{eff} of the hard spheres depends on their position in the cell. Geometrical considerations give a system of equations that links the interatomic distances with the hexagonal cell parameters a and c, as follows

$$R_A u + R_B v = \frac{\sqrt{3}}{3} a \tag{1}$$

$$R_A u + R_B w = \frac{\sqrt{a^2 + c^2}}{2} \tag{2}$$

$$R_B v + R_B w = \sqrt{\left(\frac{c}{2}\right)^2 + \left(\frac{\sqrt{3}a}{6}\right)^2} \tag{3}$$

where R^{at}_A and R^{at}_B are the atomic radius of the A and B atoms, $u = (R^{eff}_A/R^{at}_A)$, $v = (R^{eff}_{B,2c}/R^{at}_B)$, $w = (R^{eff}_{B,3g}/R^{at}_B)$. The three parameters *u*, *v* and *w* were calculated by solving the system of equations 1-3 for $MmNi_5$ considering R^{at}_{Mm} as the weighted average according to Mm composition. The values for u, v and w were assumed to be the same for the $MmNi_{5-x}Al_x$ structure. The values of parameters used in the model are summarized in table 2.

Table 2: Parameters used in the crystallographic model for $MmNi_5$.

Parameters	Values
R_{Mm} *	1.83 Å
R_{Ni} *	1.24 Å
R_{Al} *	1.43 Å
a #	4.92 Å
c #	3.99 Å
u	0.978
v	0.856
w	1.122

*[Vainshtein et al,1982] #[Esquivel and Meyer, 2007]

The substitution of Ni by Al to reach $MmNi_{5-x}Al_x$ is accounted in this model by considering $R^{at}_B = [(5-x)/5]R^{at}_{Ni} + (x/5)R^{at}_{Al}$. To that respect, the model presents no limitations. Pure lanthanide or Mm of different compositions can be replaced in the model. The model presents another advantage. The variation of cell parameters with the degree of substitution of Ni by Al can be analyzed separately depending on the B-identity substitution in each B-occupying position (2*c* and 3*g*) as shown in figure 3. It is observed (figure 3a) that the cell parameter *a* is only affected by substitutions at Wyckoff positions 2*c*, while it is not affected by substitutions in 3*g*. Furthermore, it can be seen (figure 3b) that substitutions in 2*c* and 3*g* produce a decrease and an increase in parameter *c,* respectively. It is important to note that the model predicts cell changes only for 2*c* substitution. A behavior consistent with Vegard's law, as roughly expected for replacing Ni atoms by larger Al atoms.

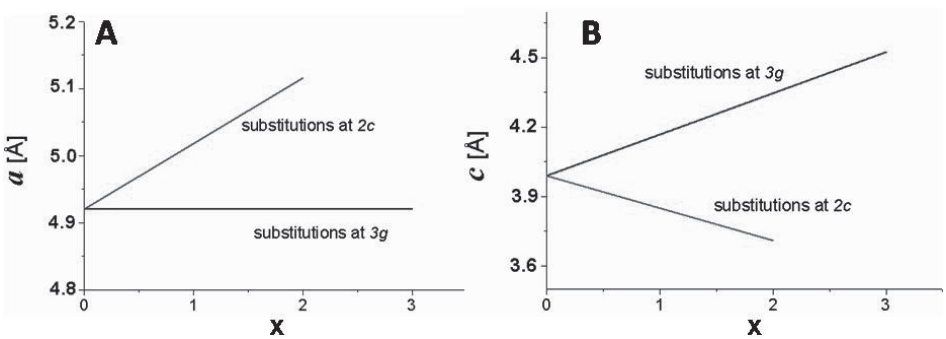

Figure 3: Variation of cell parameters of $MmNi_{5-x}Al_x$ as a function of x.

The graphs of Figure 3 allow to determine the degree of incorporation of Al in the structure from values of measured cell parameters. The following procedure is used:

• From the experimental value of *a*-cell parameter, the x´ Al content in the Wyckoff position 2*c* in figure 3*a* is calculated.

• From x´ value, the expected *c´*-cell parameter due to this partial substitution in figure 3b is determined.

• In figure 3b, the y-intercept of the line *c* vs. x at Wyckoff position 3*g* is moved to the *c´* value determined in the previous step. Then, from experimental *c*-cell parameter value, the x´´ Al content at Wyckoff position 3*g* is calculated.

• The value of x is determined as x´ + x´´.

Figure 4 shows the reduced diffractograms of samples for all nominal compositions. In this figure, peaks of $MmNi_{5-x}Al_x$ indexed as 200, 111and 002 can be seen. It is possible to observe the effect of the incorporation of Al into the structure from the shift to lower angles of the peaks which means an increase in both *a* and *c* cell parameters.

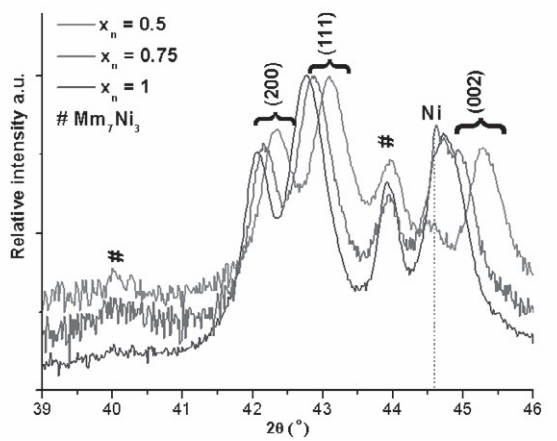

Figure 4: Reduced diffraction patterns of $MmNi_{5-x}Al_x$ for different x_n values.

On the other hand, the positions of peaks assigned to Mm_7Ni_3 appears in the same position independently of the x_n, value indicating that the same minor intermetallic phases are present in all samples.

From the extended X-ray diffractograms, cell parameters were calculated for all phases present and for each x_n. Table 2 shows the cell parameters of the minor intermetallic phases. For comparison, the theoretical values are also presented.

Table 2: Cell parameters of minor phases

Intermetallic phase	Space group	*a* [Å]		*c* [Å]	
		This work	Theoretical value*	This work	Theoretical value*
Mm_7Ni_3	$P6_3mc$	10.02 ± 0.02	10.01	6.39 ± 0.01	6.39

*Calculated as pondered average of cell parameters according to Mm composition from values for La_7Ni_3 (PDF #32-0497) and Ce_7Ni_3 (PDF #50-1256)

Then, it is concluded that Al was not incorporated in the structure of the minor intermetallic phase. Some XRD peaks of a structure corresponding to $MmNi_3$ overlap with those of $MmNi_{5-x}Al_x$ and Mm_7Ni_3. Therefore, within the detection limit or resolution of this technique, its presence cannot be discarded.

Finally, the cell parameters for intermetallics $MmNi_{5-x}Al_x$ and the corresponding x values calculated from the proposed model are summarized in table 3.

Table 3: Cell parameters and composition.

x_n	*a* [Å]	*c* [Å]	x
0.5	4.934 ± 0.004	4.013 ± 0.002	0.22
0.75	4.954 ± 0.007	4.038 ± 0.004	0.61
1	4.960 ± 0.005	4.048 ± 0.004	0.74

From the values of table 3, it is observed that the amount of Al is almost totally incorporated in the $MmNi_5$ structure for the highest x_n,

Quantitative phase analysis was performed using the direct comparison method [Waseda et al., 2011] and table 4 shows the corresponding results.

Table 4: Mass % of different phases in each sample

X_n	x	$MmNi_{5-x}Al_x$	Mm_7Ni_3	Ni
0.5	0.10	88	11	1
0.75	0.73	93	4	3
1	0.90	84	13	3

From the analysis of table 4, it is concluded that $MmNi_{5-x}Al_x$ is the main synthesis product.

4. Conclusions

An accurate determination of Al content in AB_5 structures present in mixtures of AB_5 (main)/A_7B_3(minor)/B(minor) is achieved in this work. A geometric- crystallographic model developed ad hoc allowed the accurate determination of the degree of substitution of Ni by Al for three different nominal compositions independently of the presence of secondary phases. The model was used to estimate the correct amount of Al incorporated to the sample. The model has the advantage that lanthanide compositions is not a restriction and it can be extended to other B-type elements (Co, Sn, Zn) provided the atomic radius is available. This result is relevant because a usual-widely available structural technique such as XRD is used to accurately estimate the degree of substitution of the alloying elements in the AB_5 structure without the need of elemental determination techniques. This feature is also needed when the hydrogen absorption properties have to be correlated with the precise composition of AB_5 intermetallic in the design of multistage hydrogen thermal compressors.

Acknowledgements

S. A. Obregón thanks the PRH-PDFT-200-4 program of CNEA and ANPCyT of Argentina for the PhD grant. The authors thank CONICET of Argentina (Project PIP No. 0109) and CNEA of Argentina for partial financial support.

The authors wish to thank the reviewer for the helpful comments and careful revision of the manuscript.

References

Ares J. R., Cuevas F., Percheron-Guegán A., 2005, Microstructural effects in the hydrogenation kinetics of commercial-type $LaNi_5$ alloy. Journal of Alloys and Compounds 404-406, p 327.

Esquivel, M.R., Meyer, G., 2007, A comparison of the evolution during the mechanical alloying of both a $MmNi_5$–Ni and a Mm–Ni mixtures: Stages of milling and microstructural characterization, Journal of Alloys and Compounds 446-447, p 212.

Esquivel, M.R, Rodriguez, M.G, 2009, Integral treatment for materials applied to a linking stage between low (1-600) kPa and high (2100-3000 kPa) pressures in hydrogen thermal compression schemes, Energy Materials: science and engineering for energy systems 4, p 145.

Jurczyk, M., Nowak, M. Jankowska, E., 2002, Nanocrystallyne $LaNi_{4-x}Mn_{0.75}Al0.25Co_x$ electrode materials prepared by mechanical alloying ($0<x<1.0$), Journal of Alloys and Compounds 340 , p 281.

Koch, C.C., Whittenberger J.D., 1996, Review on Mechanical milling/alloying of intermetallics, Intermetallics 4 , p 339.

Langford J.I., Delhez, R.D.E., Keijser, T.H.H., Mittemeijer, E.J. 1988, Profile analysis for microcrystalline properties by the Fourier and other methods. Australian Journal of Physics 41, p 173

Liang, G., Huot, J., Schultz, R., 2001, Hydrogen storage properties of mechanically alloyed $LaNi_5$-based materials, Journal of Alloys and Compounds 320 , p 133.

Magee, C.B., Liu, J., Lundin, C.E., 1981, Relationship between intermetallic compound structure and hydride formation, Journal of less common metals 78, p 119.

Mediema, A.R., Buschow, K. H. J., Van Mal, H.H., 1983, Which intermetallic compounds of transition metals form stable hydrides?, Journal of less common metals 91, p 1.

Obregón S. A., Andrade Gamboa J. J., Esquivel M. R.;2012, Synthesis of Al-containing $MmNi_5$ by mechanical alloying:milling stages, structure parameters and thermal annealing.: International Journal of Hydrogen Energy, In Press, doi:10.1016/j.ijhydene.2012.01.170.

Simičić, M.V., Zdujić, M., Jelovac, D.M., Rakin, P.M., 2001, Hydrogen storage material based on $LaNi_5$ alloy produced by mechanical alloying, Journal of power sources 92, p 250.

Suryanarayana, C, 2001, Mechanical alloying and milling, Progress in material science 46,p 1.

Vainshtein B.K., Fridkin V.M., Indenbom V.L., 1982, Modern crystallography II: Structure of crystals, Berlin Heidelberg: Springer-Verlag, p 71.

Waseda Y., Matsubara E., Shinoda K, 2011, X-Ray Diffraction Crystallography Introduction, Examples and Solved Problems, Berlin Heidelberg: Springer-Verlag, p 153.